# Transient Photoligation Behavior of Nickel Protoporphyrin Reconstituted Myoglobin and Hemoglobin

**ARTICLE** *in* JOURNAL OF THE AMERICAN CHEMICAL SOCIETY · JULY 1986

Impact Factor: 12.11 · DOI: 10.1021/ja00274a026



**4 AUTHORS**, INCLUDING:

John A Shelnutt
University of Georgia
**265** PUBLICATIONS **8,720** CITATIONS

SEE PROFILE

Mark R Ondrias
University of New Mexico
**118** PUBLICATIONS **2,185** CITATIONS

SEE PROFILE

required for agreement between their observed and calculated spectra. Our conclusion that this Gaussian feature is an integral part of the $S_2$ state multiline EPR spectrum, and not due to background interference, is further supported by our observation that it exhibits the same temperature dependence and microwave power saturation behavior as the sharper features of the spectrum (data not shown).

It is important to point out that a $Mn^{III}$–$Mn^{IV}$ dimer model can only be successful in simulating the EPR spectrum of the $S_2$ state produced from the untreated resting state by 200 K illumination. The results of Table II show that the other $S_2$ state multiline EPR signals have considerable tetramer character and, consequently, the $Mn^{III}$–$Mn^{IV}$ dimer approximation of the $^{55}Mn$ nuclear hyperfine coupling becomes invalid.

## Conclusions

In this contribution, we advance a model for the $S_2$ state of the OEC where two antiferromagnetically exchange coupled Mn dimers are ferromagnetically exchange coupled. Both the magnetic properties and the $^{55}Mn$ nuclear hyperfine couplings of five distinct $S_2$ state EPR signals can be satisfactorily explained by this model.

The simulation parameters in Table I indicate that both large antiferromagnetic and ferromagnetic exchange couplings are needed to explain the temperature dependence and microwave power saturation behavior of the $S_2$ state EPR spectra. Even though large ferromagnetic exchange couplings are not commonly found in synthetic complexes, a few examples do exist.[18] There is also ample precedent in the literature of tetrameric complexes where both large antiferromagnetic and large ferromagnetic exchange interactions occur simultaneously, such as $Cu_4O_4$ cubane-like clusters[13] and the $Fe_4S_4$ centers of ferredoxins.[12] The analogies which can be made with the $Cu_4O_4$ and $Fe_4S_4$ cubane-like complexes prompt us to speculate that the Mn site of the OEC exists as a $Mn_4O_4$ cubane-like structure in the $S_2$ state.

**Acknowledgment.** This work was supported by the National Institutes of Health (GM32715), the Chicago Community Trust/Searle Scholars Program, the Camille and Henry Dreyfus Foundation, and a National Science Foundation Graduate Fellowship to W.F.B.

# Transient Photoligation Behavior of Nickel Protoporphyrin Reconstituted Myoglobin and Hemoglobin†

**E. W. Findsen,‡ K. Alston,§ J. A. Shelnutt,⊥ and M. R. Ondrias*†**

*Contribution from the Department of Chemistry, University of New Mexico, Albuquerque, New Mexico 87131, Department of Natural Sciences, Benedict College, Columbia, South Carolina 29204, and the Solid State Materials Division, Sandia National Laboratories, Albuquerque, New Mexico 87185.* *Received January 9, 1986*

**Abstract:** The transient photoligation behavior of nickel protoporphyrin IX (Ni(PP)) in a variety of local environments has been studied by time-resolved resonance Raman scattering. In coordinating basic solvents the ligation changes engendered by the photoexcitation of a net $d^2_{z^2} \rightarrow d^1_{x^2-y^2}, d^1_{z^2}$ ($^1A_{1g} \rightarrow {}^3B_{1g}$) transition are easily monitored by changes in Ni(PP) Raman modes that are sensitive to metalloporphyrin spin-state and ligation changes. The Raman results for those systems corroborate the photochemical cycle and excited state lifetimes proposed by Holten and co-workers (*Chem. Phys.* **1983**, *75*, 305). However, the photodynamics exhibited by Ni(PP) incorporated into Mb or Hb apoproteins or into detergent micelles are distinct from those of Ni(PP) in coordinating solvents and from each other. The equilibrium 4-coordinate Ni(PP) sites in NiHb display a transient photoassociation of a single ligand (most likely the proximal histidine) similar to the behavior of Ni(PP) in solution. The photodynamics of the equilibrium 5-coordinate Ni(PP) sites in NiHb and NiMb are, however, greatly modulated by the surrounding protein matrix. The major effects of the protein environment are concluded to be the stabilization of the ligand binding transition states thus facilitating photoassociation of the proximal histidine at the 4-coordinate site and enhancing the recombination rate of the photodissociated histidine at the 5-coordinate sites. In a hydrophobic micellar environment where no potential axial ligands are present, photoexcitation of 4-coordinate Ni(PP) results in the direct observation of the resonance Raman spectrum of the unligated $^3B_{1g}$ state. This allows for the deconvolution of the effects upon the porphyrin of the excited-state spin-state transition from those produced by ligation.

The metalloporphyrins are a diverse class of complex molecules that display a wide variety of photochemical and metal ligand binding behavior.[1-3] They are of interest as potential catalysts and photosensitizing agents as well as for understanding the key role that metalloporphyrins play in biological processes. Moreover, the chemical properties of specific metalloporphyrins are signicantly altered when they are incorporated into a protein matrix. The pervasive influence of the protein environment upon the equilibrium properties of metalloporphyrin active sites is well-documented for a wide variety of systems.

Recently, transient optical techniques have demonstrated that the dynamic behavior of active sites in hemoproteins is similarly predicted to a large degree upon its immediate protein environment.[4-7] Transient resonance Raman scattering has proven

† This work was performed at the University of New Mexico and supported by the National Institutes of Health (GM33330), the donors of the Petroleum Research Fund, administered by the American Chemical Society (to M.R.O.), The U.S. Department of Energy (Contract DE-AC04-76DP00789), the Gas Research Institute (Contract No. 5082-260-0767 (to J.A.S.)), and the graduate research scholarship fund of the Associated Western Universities (to E.W.F.).

‡ University of New Mexico.
§ Benedict College.
⊥ Sandia National Laboratories.

(1) *The Porphyrins*; Dolphin, D., Ed.; Academic Press: New York, 1978–1983; Vol. 1–8.
(2) *Iron Porphyrins*; Lever, A. B. P., Gray, H. B., Eds.; Addison-Wesley: Reading, PA, 1983; Vols. 1 and 2.
(3) *Porphyrins and Metalloporphyrins*; Smith, K. M., Ed.; Elsevier: New York, 1975.
(4) Friedman, J. M.; Ondrias, M. R.; Rousseau, D. L. *Annu. Rev. Phys. Chem.* **1982**, *33*, 471.
(5) Spiro, T. G. In *Iron Porphyrins*; Lever, A. B. P., Gray, H. B., Eds.; Addison-Wesley: Reading, PA, 1983; Vol. 2, p 89.
(6) Debunner, P. G.; Frauenfelder, H. *Annu. Rev. Phys. Chem.* **1982**, *33*, 283.

0002-7863/86/1508-4009$01.50/0 

particularly well-suited for exogenous ligand binding studies because of its inherent specificity toward the chromophore and its large structural information content.[4,5]

One reason for the current interest in nickel porphyrin reconstituted hemoproteins is that the nickel porphyrin provides a useful reporter group for conformation changes at the active site. The simplicity of the bonding of nickel to the macrocycle and to axial ligands facilitates the interpretation of spectroscopic results. Further, nickel reconstituted proteins do not bind exogeneous ligands such as CO and $O_2$; thus, they provide useful model systems for selectively investigating the dynamics of ligation of basic ligands provided by the protein itself. Investigation of nickel reconstituted hemoproteins is also of direct biological importance for understanding protein interactions with the nickel tetrapyrrole ($F_{430}$) in the active site of methylreductase—an enzyme involved in $CO_2$ fixation by methanogenic bacteria.[8]

In this study we document the transient photoinduced ligation changes exhibited by the active sites of nickel protoporphyrin reconstituted myoglobin (NiMb) and hemoglobin (NiHb).

Previous transient absorption studies[9-12] have elucidated the spin state and ligation changes occurring in nickel octaethylporphyrin (OEP), tetraphenylporphyrin (TPP), mesoporphyrin (MesoP), protoporphyrin IX (PP), and protoporphyrin dimethyl ester (PPDME) in coordinating and noncoordinating solvents. The nickel porphyrins in coordinating solvents generally exist as equilibrium mixtures of 4- and 6-coordinate species possessing distinctive absorption spectra. It was found that the absorption of a photon by nickel porphyrins in coordinating solvents results in either the photolysis of axial ligands (if the ground state was 6-coordinate) or the photoinduced ligation of solvent molecules (if the ground state was 4-coordinate). This behavior was explained on the basis of photoinduced changes in metal spin state ($d^1_{z^2}$, $d^1_{x^2-y^2} \leftrightarrow d^2_{z^2}$) and its concomitant effect upon porphyrin–ligand electronic interactions.

A recent transient Raman study[13] of Ni(OEP) in coordinating and noncoordinating solvents has corroborated this scenario and probed the effects of photoinduced ligation/deligation upon the metalloporphyrin vibrational properties. In this work, we have extended the transient Raman studies to Ni(PP) and Ni(PPDME) in coordinating and noncoordinating solvents and micellar solutions. The nickel protoporphyrins exhibit photoligation processes similar to the analogous Ni(OEP) models.

For our purposes, the nickel porphyrins and nickel protoporphyrin reconstituted globins are nearly ideal systems for study by Raman techniques. In addition to the transient absorption and Raman studies of Ni(OEP) complexes, a resonance Raman investigation of the equilibrium forms of NiMb and NiHb has recently been completed.[14,15] The equilibrium Raman results showed that NiHb has two different types of nickel protoporphyrin sites. One site contains 4-coordinate nickel protoporphyrin by analogy to nickel protoporphyrin in noncoordinating solvents. The other site in NiHb was very similar to that of NiMb, and both possess Raman spectra quite different from 4- or 6-coordinate model nickel protoporphyrin complexes. The Raman modes of the porphyrin ring in these sites were consistent with 5-coordination. The identification of the nickel ligand stretching mode at 236 $cm^{-1}$ via $^{64}Ni$ isotopic substitution suggests that imidazole is the single axial ligand at the 5-coordinate sites. The 5-coordinate complex is apparently unique to the reconstituted protein as 5-coordinate model nickel porphyrins exist only at very low concentration in solution and have not been observed directly.[16]

The transient Raman data reported here indicate that the behavior of the nickel protoporphyrin sites in NiHb and NiMb is unique from nickel porphyrin model complexes. Despite the fact that the 6-coordinate nickel protoporphyrin in coordinating solvents releases both ligands upon photoexcitation, we find no evidence for photoinduced axial ligand release (on a 10-ns time scale) in NiMb or the 5-coordinate NiHb sites. The 4-coordinate NiHb sites, on the other hand, are photoactive and become transiently 5-coordinate subsequent to excitation.

This work expands the study of these transient photoprocesses into the biophysical domain. Previous transient Raman studies[4,5,17-29] of native (iron protoporphyrin containing) proteins have determined the metastable heme geometries resulting from the photolysis of exogenous (CO, $O_2$, NO) sixth ligands. However, no evidence, even on a picosecond time scale,[20-23] was found for the photolysis of the nitrogenous ligand supplied by the protein and occupying the fifth ligation position. On the other hand, photoinduced release of the fifth axial ligand was anticipated in the nickel protoporphyrin reconstituted proteins (by analogy to the behavior of the nickel porphyrin models). Thus, the apparent absence of ligand ejection on a nanosecond time scale in the nickel reconstituted globins demonstrates an impressive effect of the protein matrix. Moreover, differences in the electronic and vibrational response of metalloporphyrins subsequent to photoexcitation could provide additional insight into the perturbations of metalloporphyrin function by a specific protein environment.

## Materials and Methods

Nickel protoporphyrin was obtained from Porphyrin Products (Logan, UT) and used without further purification. NiMb and NiHb were prepared from sperm whale myoglobin and human adult hemoglobin as described by Alston and Storm.[30] Each was in 50 mM phosphate buffer at pH 7.5. Pyrrolidine was obtained from Aldrich Chemical Co. (Gold Label) and used without further purification. The detergents CTAB (cetyltrimethylammonium bromide) and SDS (sodium dodecyl sulfate) were used as received from Sigma Chemical Co. and American Biochemical Co., respectively. Samples were contained in either a quartz EPR tube (Wilmad) or a quartz cuvette. The samples were not deoxygenated because previous equilibrium Raman and UV–vis absorption studies showed no effect due to the presence of oxygen. All spectra were obtained at room temperature (~20–25 °C).

The transient Raman spectra were obtained with use of a Molectron UV-24 and a Molectron DL-24 laser system (10 ns nominal pulse width). The output laser beam was imaged on the sample in a back scattering geometry with either a spherical or cylindrical lens. The scattered radiation was then focused into a SPEX Industries Model 1403 scanning double monochromator. The output from the monochromator was detected with use of an Hamamatsu R928 photomultiplier tube (PMT) in a cooled housing. The output of the PMT was directed into an EG& G/PAR Model 162 boxcar with a single plug-in (Model 165). The

(7) Noe, L. In *Biological Events Probes by Ultrafast Laser Spectroscopy*; Alfano, R., Ed.; Academic Press: New York, 1982; p 339.
(8) Pfaltz, A.; Jaun, B.; Fassler, A.; Eschenmaser, A.; Jaechen, R.; Gilles, H.-H.; Diekart, G.; Thauer, R. K. *Helv. Chim. Acta* **1982**, *65*, 825.
(9) Kim, D.-H.; Kirmaier, C.; Holten, D. *Chem. Phys. Lett.* **1983**, *98*, 584.
(10) Kim, D.-H.; Holten, D. *Chem. Phys.* **1983**, *75*, 305.
(11) (a) Holten, D.; Gouterman, M. In *Proceedings of the Symposium on Optical Properties and Structures of Tetrapyrroles*; Kunstanz, 1984. (b) Kobayashi, T.; Straub, K.; Rentzpeis, P. M. *Photochem. Photobiol.* **1979**, *29*, 925.
(12) Chirvonyi, V. S.; Dzhagarov, B. M.; Timinskii, Y. V.; Gurinovich, G. P. *Chem. Phys. Lett.* **1980**, *70*, 79.
(13) Findsen, E. W.; Shelnutt, J. A.; Friedman, J. M.; Ondrias, M. R. *Chem. Phys. Lett.*, in press.
(14) Shelnutt, J. A.; Alston, K.; Ho, J.-Y.; Yu, N.-T.; Yamamoto, T.; Rifkind, J. M. *Biochemistry*, **1985**, *25*, 620.
(15) Shelnutt, J. A.; Alston, K.; Findsen, E. W.; Ondrias, M. R.; Rifkind, J. M. *Proceedings of the International Conference on Excited States and Dynamics of Porphyrins*; in press.
(16) LaMar, G. N.; Walker, F. A. In *The Porphyrins*; Dolphin, D., Ed.; Academic Press: New York, 1979; p 61.
(17) Friedman, J. M.; Stepnoski, R. A.; Stavola, M.; Ondrias, M. R.; Cone, R. *Biochemistry*, **1982**, *21*, 2022.
(18) Scott, T. W.; Friedman, J. M. *J. Am. Chem. Soc.* **1984**, *106*, 5677.
(19) Ondrias, M. R.; Friedman, J. M.; Rousseau, D. L. *Science* **1983**, *220*, 614.
(20) Findsen, E. W.; Friedman, J. M.; Scott, T. W.; Chance, M. R.; Ondrias, M. R. *J. Am. Chem. Soc.* **1985**, *107*, 3355.
(21) Findsen, E. W.; Friedman, J. M.; Ondrias, M. R.; Simon, S. R. *Science* **1985**, *228*, 661.
(22) Dasgupta, S.; Spiro, T. G.; Johnson, C. K.; Dalikas, G. A.; Hochstrasser, R. M. *Biochemistry* **1985**, *24*, 5295.
(23) Terner, J.; Stong, J. D.; Spiro, T. G.; Nagumo, M.; Nicol, M. F.; El-Sayed, M. A. *Proc. Natl. Acad. Sci. U.S.A.* **1981**, *78*, 1313.
(24) Ondrias, M. R.; Scott, T. W.; Friedman, J. M.; MacDonald, V. W. *Chem. Phys. Lett.* **1984**, *112*, 351.
(25) Woodruff, W. H.; Farquhausan, S. *Science* **1978**, *201*, 183.
(26) Irwin, M. J.; Atkinsen, G. H. *Nature (London)* **1981**, *293*, 37.
(27) Babcock, G. T.; Jean, J. M.; Johnson, L. N.; Palmer, G.; Woodruff, W. H. *J.* Am. *Chem. Soc.* **1984**, *106*, 8305.
(28) Alden, R. G.; Ondrias, M. R. *J. Biol. Chem.* **1985**, *260*, 12194.
(29) Findsen, E. W.; Ondrias, M. R. *J. Am. Chem. Soc.* **1984**, *106*, 5736.
(30) Alston, K.; Storm, C. B. *Biochemistry* **1979**, *18*, 4292.

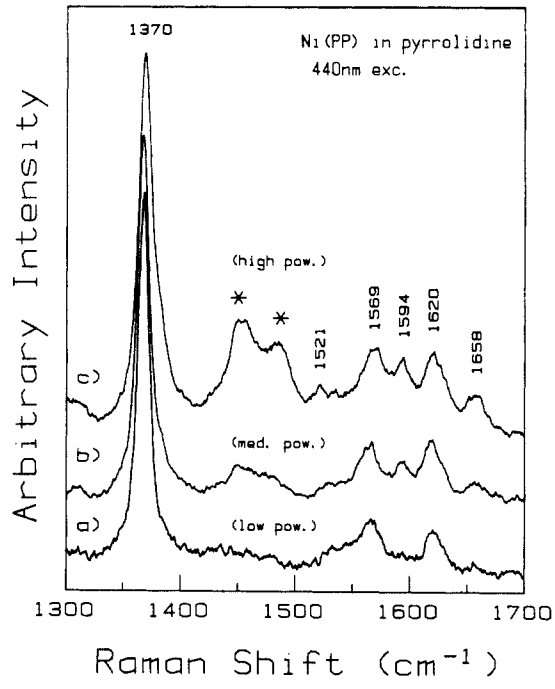


**Figure 1.** Resonance Raman spectra of nickel protoporphyrin IX in pyrrolidine with 440-nm excitation. Spectrum a was obtained at low photon density by defocusing the cylindrical lens which directs the laser beam onto the sample. Spectrum b was obtained with the same conditions as in spectrum a except that the cylindrical lens was positioned such that a very sharp laser beam was imaged at the sample. To obtain spectrum c the cylindrical lens was replaced with a sharply focused spherical objective resulting in an approximately 10× higher photon density at the sample. In all spectra shown the spectral band-pass is 7–9 $cm^{-1}$. Solvent bands are denoted by an asterisk.

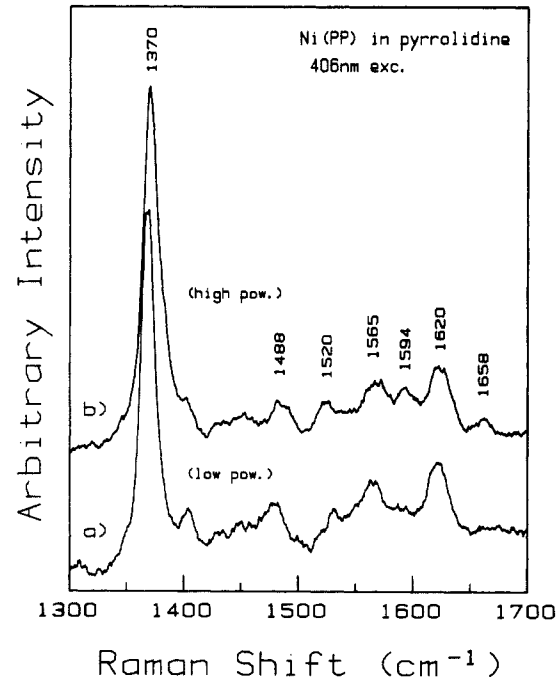


**Figure 2.** Resonance Raman spectra of nickel protoporphyrin IX in pyrrolidine obtained with 406-nm excitation. Spectrum a was obtained at low photon density (low power), using a very defocused cylindrical lens to image the laser beam on the sample. The average laser power was ~0.75 mW at ~9 Hz. For spectrum b the average laser power was ~6 mW at 9 Hz, and a spherical lens was used to focus the beam tightly onto the sample. The photon density for the high-power spectra was ~40× higher than in the low-power spectra.

boxcar signal was then fed into a Datamate Controller (SPEX) which controlled the monochromator as well as stored the data points accumulated.

Laser power densities at the sample were controlled by the beam focusing optics or the use of neutral density filters. Unless otherwise noted, low-power spectra were obtained with a cylindrical lens which delivered ~10 $mJ/cm^2$ and very high power spectra with a spherical lens which produced 75–300 $mJ/cm^2$, depending upon its focal position. In all spectra, the spectral band-pass was 7–9 $cm^{-1}$, depending on excitation wavelengths.

## Results

Raman spectra of the various Ni(PP) species studied in this work are presented in Figures 1–6. Table I is a compilation of the positions of the Raman modes of interest, conditions under which they were obtained, and the dominant ligation state of the various species.

For nickel protoporphyrin in pyrrolidine, the spectrum (see Figures 1 and 2) observed under low-power conditions is that of the 6-coordinate species with the axial positions of the metal in the porphyrin macrocycle occupied by the pyrrolidine (solvent) molecules. In the low-power spectra of Figures 1 and 2, $^6\nu_2$, $^6\nu_3$, and $^6\nu_{10}$ occur at 1566, 1486, and 1618 $cm^{-1}$, respectively, which are positions exhibited by equilibrium 6-coordinate forms [14,15] of nickel protoporphyrin. (The designation of porphyrin skeletal modes follows that of Abe et al. (J. Chem. Phys. (1978) *69*, 4526) and uses the nomenclature $^m\nu_n$ to denote the $n$th normal mode of the $m$-coordinate species and $^*\nu_n$ to denote the $n$th mode of the unligated $B_{1g}$ excited state of Ni(PP). Our mode assignments follow those of Choi et al.[31]) At higher powers, peaks at 1591, 1520, and 1657 $cm^{-1}$ become evident. These are attributed to $^4\nu_2$, $^4\nu_3$, and $^4\nu_{10}$, respectively, of 4-coordinate Ni(PP). The shoulder observed near 1630 $cm^{-1}$ is most likely the peripheral vinyl stretching vibration[31] of the 4-coordinate Ni(PP) species. Similar spectral changes are observed with both 420- and 406-nm excitation.

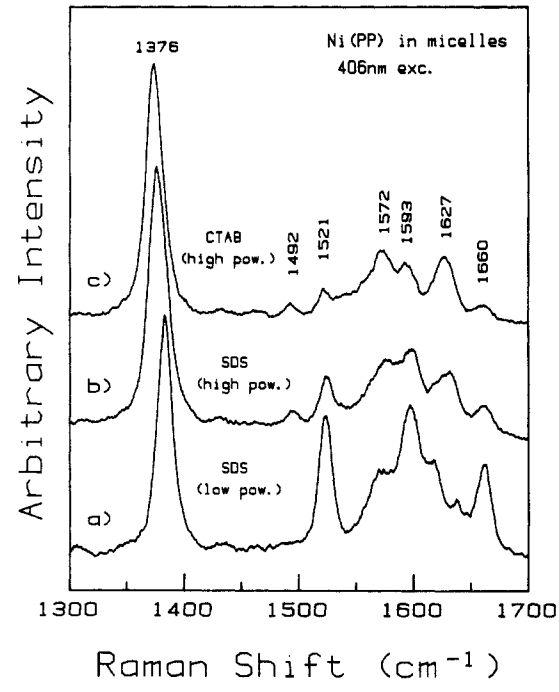


**Figure 3.** Resonance Raman spectra of nickel protoporphyrin IX incorporated into micelles of sodium dodecyl sulfate (SDS) and cetyltrimethylammonium bromide (CTAB) at detergent concentrations of 2.48 and 1.2 mg/mL, respectively. Spectrum a was obtained at low photo density with 406-nm excitation with SDS as the detergent. The low photon density spectrum obtained from Ni(PP) in CTAB was identical with that of Ni(PP) in SDS, and both are characteristic of the 4-coordinate ground state. Spectra b and c were obtained from Ni(PP) in SDS and CTAB, respectively, at high photon density with 5 mW average power (~9 Hz) and a laser beam sharply focused via a spherical lens.

(31) Choi, S.; Spiro, T. G.; Langry, K. C.; Smith, K. M. *J. Am. Chem. Soc.* **1982**, *104*, 4337.

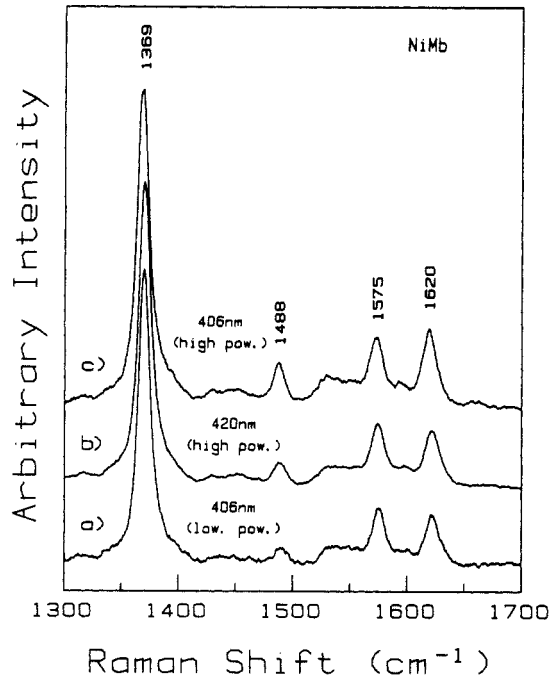


**Figure 4.** The spectra obtained from nickel reconstituted myoglobin with low and high photon densities and different excitation frequencies are shown. Spectrum a was obtained from NiMb in 50 mM phosphate buffer, pH ~7.5, at low photon densities. With 420-nm excitation, the low photon density spectra were obtained with use of a very defocused laser beam with an ~1.5 mW average power at ~10 Hz. High photon density spectra were obtained with ~8 mW average laser power which was tightly focused via a spherical lens. Spectra b and c were obtained at high photon density with 420- and 406-nm excitation, respectively. The spectra illustrate the lack of spectral changes even when excitation is used which should enhance the excited state species if it is formed. The weak peaks observed at the position characteristic of the 4-coordinate species are observed at the same relative intensity with use of low photon density with 406-nm excitation. This small amount of the 4-coordinate species is due to a fraction (<10%) of the sample which is 4-coordinate in the ground state.

Nickel protoporphyrins in micelles have been shown to be 4-coordinate at equilibrium.[14] Thus, they provide model systems for monomeric Ni(PP) in a noncoordinating hydrophobic environment. In Figure 3 the spectra of nickel protoporphyrin incorporated into SDS micelles are shown for low and high power. Also shown are the spectra obtained with high laser powers for Ni(PP) incorporated into CTAB micelles. Both detergents yield similar low-power Ni(PP) spectra. The high-power spectra are radically different from the low-power spectra and also dissimilar to those obtained for the 6-coordinate complex of Ni(PP) in piperidine. Explanation of this behavior follows in the discussion.

The resonance Raman spectra of NiMb (Figure 4) present a distinct contrast to those of the model nickel protoporphyrin systems. The Raman spectrum observed with 420-nm excitation is that associated with the 5-coordinate state. The modes $^5\nu_4$, $^5\nu_3$, $^5\nu_2$, and $^5\nu_{10}$ occur at 1370, 1489, 1576, and 1618 cm$^{-1}$, respectively. At very high powers and 420-nm excitation, slight changes (within the ±2-cm$^{-1}$ accuracy of this study) in the positions of 5-coordinate modes $^5\nu_4$, $^5\nu_3$, and $^5\nu_{10}$ were evident, but no new bands characteristic of either the 4-coordinate or 6-coordinate forms were observed. Similar behavior was also observed with 406-nm excitation. Therefore, no photoinduced ligation changes are observed for NiMb regardless of the power density or excitation wavelength.

The most interesting system studied is NiHb. At equilibrium it is a mixture (60:40) of 4- and 5-coordinate forms.[32-34] By using

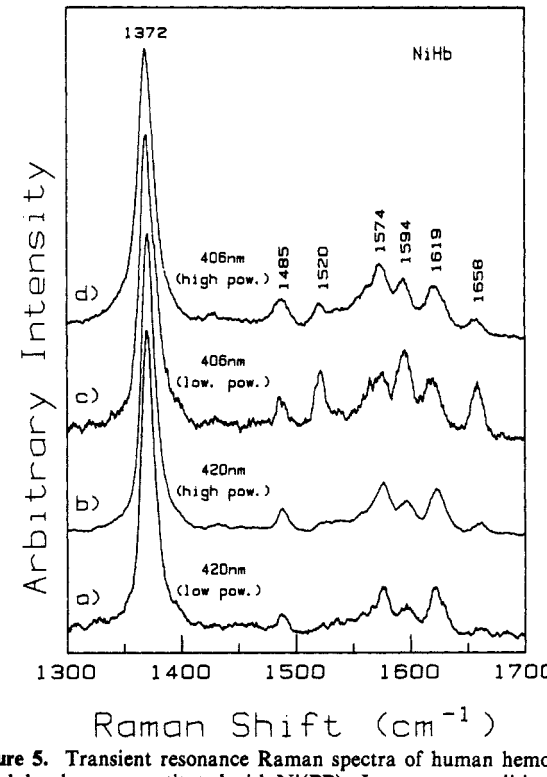


**Figure 5.** Transient resonance Raman spectra of human hemoglobin which has been reconstituted with Ni(PP). Instrument conditions were the same as those used in Figure 4. Spectrum a was obtained with 420-nm laser excitation at low photon density. High photon density was used to obtain spectrum b. Spectra c and d were obtained with use of 406-nm excitation at low and high photon densities, respectively.

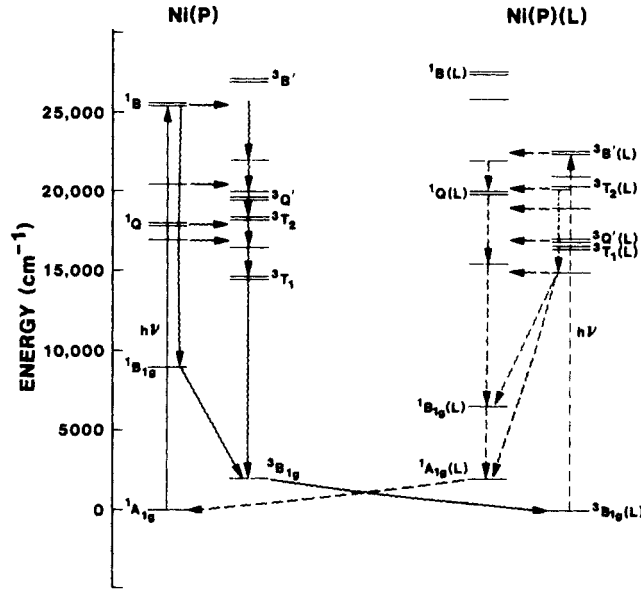


**Figure 6.** Relaxation pathways leading to ligand photodissociation (dashed) and ligand binding (solid). Singlet and triplet state energies are for unligated (left) and ligated (right) nickel porphyrins. Other pathways exist for ground-state recovery. Excited-state deactivation and thermal ligand binding and loss are not shown. The energies are taken from the calculations of Ake and Gouterman[35] for (in-plane) 4-coordinate nickel porphine and (out-of-plane) 5-coordinate nickel porphine with a pyridine ligand. The $^3B_{1g}$–$^1A_{1g}$ energy gap was taken to be 2000 cm$^{-1}$ for Ni(PP)(L). We have also set the ground states ($^1A_{1g}$ for 4-coordinte, $^3B_{1g}$(L) for 5-coordinate form) equal since they are in equilibrium for the systems we have studied. States labeled Q, B, $T_1$, $T_2$ are $\pi \rightarrow \pi^*$ states; $A_{1g}$ and $B_{1g}$ are metal states of the porphyrin ground state.

420-nm excitation at low power modes of each form are observed (Table I) in approximately their equilibrium intensity ratios (see Figure 5). At high powers the spectrum remains unchanged except for a possible small shift in $\nu_4$ to higher frequency.

(32) Alston, K.; Park, C. M.; Rodgers, D. W.; Edelstein, S. J.; Nagel, R. L. *Blood* **1985**, *64*, Part II, 556.
(33) Manoharan, P. T.; Alson, K.; Rifkind, J. M. *Bull. Magn. Reson.* **1983**, *5*, 255.
(34) Manoharan, P. T.; Alston, K.; Rifkind, J. M. In *Copper Coordination Conference Proceedings*; Albany, NY, in press.

**Table I**[a]

Ni(PP) in Pyrrolidine

| | high-frequency Raman bands ($cm^{-1}$) | | | |
|---|---|---|---|---|
| | 406 nm | | 440 nm | |
| | low power | high power | low power | high power |
| $^6\nu_4$ | 1368 | 1370 | 1368 | 1370 |
| $^4\nu_4$ | | | | |
| $^6\nu_3$ | 1480 | 1488 | 1480 | 1484 |
| $^4\nu_3$ | | 1520 | | 1521 |
| $^6\nu_2$ | 1565 | 1569 | 1565 | 1569 |
| $^4\nu_2$ | | 1595 | | 1594 |
| $^6\nu_{10}$ | 1620 | 1625 | 1620 | 1620 |
| $^4\nu_{10}$ | | 1658 | | 1658 |

Ni(PP) in CTAB and SDS Micelles (406-nm Excitation)

| | Raman frequencies ($cm^{-1}$) | | | |
|---|---|---|---|---|
| | CTAB | | SDS | |
| | low power | high power | low power | high power |
| $^4\nu_4$ | 1383 | 1374 | 1384 | 1376 |
| $^*\nu_4$ | | | | |
| $^4\nu_3$ | 1524 | 1521 | 1523 | 1524 |
| $^*\nu_3$ | | 1492 | | 1495 |
| $^4\nu_2$ | 1596 | 1593 | 1597 | 1598 |
| $^*\nu_2$ | | 1572 | | 1577 |
| $^4\nu_{10}$ | 1660 | 1660 | 1662 | 1661 |
| $^*\nu_{10}$ | | 1627 | | 1632 |

NiMb in 50-nm Phosphate

| | Raman frequencies ($cm^{-1}$) | | | | | |
|---|---|---|---|---|---|---|
| | 420 nm | | 406 nm | 406 nm | | 413 nm |
| | low power | high power | cw | low power | high power | cw |
| $^5\nu_4$ | 1370 | 1370 | 1368 | 1370 | 1369 | 1368 |
| $^5\nu_3$ | 1487 | 1489 | 1487 | 1487 | 1488 | 1487 |
| $^5\nu_2$ | 1575 | 1574 | 1572 | 1575 | 1575 | 1572 |
| $^5\nu_{10}$ | 1621 | 1621 | 1619 | 1621 | 1620 | 1619 |

NiHb in 50 mM Phosphate

| | Raman frequencies ($cm^{-1}$) | | | | |
|---|---|---|---|---|---|
| | 406 nm | | 420 nm | | 407 nm |
| | low power | high power | low power | high power | cw |
| $^5\nu_4$ | 1369 | 1369 | 1371 | 1372 | 1367 |
| $^4\nu_4$ | | | | | |
| $^5\nu_3$ | 1486 | 1488 | 1487 | 1488 | 1485 |
| $^4\nu_3$ | 1522 | 1521 | 1522 | 1521 | 1520 |
| $^5\nu_2$ | 1575 | 1574 | 1575 | 1577 | 1574 |
| $^4\nu_2$ | 1595 | 1594 | 1597 | 1597 | 1594 |
| $^5\nu_4$ | 1619 | 1621 | 1622 | 1623 | 1619 |
| $^4\nu_{10}$ | 1659 | 1657 | 1622 | 1662 | 1658 |

[a] An asterisk denotes the species formed from the excited state which has $B_{1g}$ character.

However, with 406-nm excitation (which preferentially excites the 4-coordinate sites), changes are observed between the spectra obtained at high and low power. Most noticeable is that the intensities of $^4\nu_2$, $^4\nu_3$, and $^4\nu_{10}$ are drastically decreased in the high-power spectrum relative to those of $^5\nu_2$, $^5\nu_3$, and $^5\nu_{10}$. This clearly indicates that the 4-coordinate ground-state sites of NiHb are photoactive whereas the 5-coordinate sites are not (at least on a nanosecond time scale).

## Discussion

In this work Ni(PP) has been probed in the 4-, 5-, and 6-coordinate ground states both in solution and incorporated into micelles or a protein matrix. The photochemical behavior of the 4- and 6-coordinate Ni(PP) species in solution closely parallels the previously observed behavior of analogous Ni(OEP) species. The stability of the 5-coordinate state in NiMb and NiHb is apparently due to the unique influence of the protein. The ability of the protein environment to stabilize a generally unfavorable conformation is direct evidence for modulation of heme properties by its immediate environment. The fact that NiMb is almost completely 5-coordinate whereas NiHb is a mixture which has a large 4-coordinate component demonstrates the more subtle influence on the heme by local hemepocket conformational differences between the two proteins. Our data establish that photoinduced ligation behavior of Ni(PP) is also significantly modulated by protein influences.

**Nickel Porphyrin Photodynamics.** A second theoretical basis for the interpretation of the photoligation behavior of metalloporphyrins in solution has already been established. Molecular orbital calculations on nickel porphine by Ake and Gouterman[35] have estimated the relative energies of the available charge-transfer and d–d transitions for nickel porphyrins in various states of ligation (see Figure 6). These have, in turn, been used to explain the time scales of the transient absorption changes observed in these species.[9,10] The rate-limiting steps in the photocycle were concluded to be d–d transitions involving spin-state changes at the metal.

Molecular orbital calculations[35] indicate that the $d^8$ nickel ion in nickel porphyrins is in an $^1A_{1g}$ state when 4-coordinate, with

(35) Ake, R. L.; Gouterman, M. *Theor. Chim. Acta* **1970**, *17*, 408.

paired electrons in the $d_{xy}$, $d_{yz}$, $d_{xz}$ orbitals, as well as the $d_{z^2}$ orbital. In the 6-coordinate ligation state the $d_{z^2}$ orbital is destabilized with respect to the $d_{x^2-y^2}$ orbital due to the proximity of the electron rich (basic) axial ligand. This destabilization causes the promotion of one of the $d_{z^2}$ electrons to the $d_{x^2-y^2}$ orbital. Now two electronic states are possible, the $^3B_{1g}$ state and the $^1B_{1g}$ state with the triplet at lower energy. Both the 5- and 6-coordinate forms can stabilize the $^3B_{1g}$ state. In the 6-coordinate form nickel is in an octahedral environment and therefore is in the porphyrin plane, whereas the 5-coordinate form may have the nickel slightly out of plane.

Picosecond transient absorption measurements,[9,10] as well as transient Raman studies,[13] have shown that when Ni(OEP) in a highly coordinating solvent such as piperidine is excited by a photolytic pulse of high energy, the ligation state of the transient species is different from that of the ground state. At equilibrium, both 4- and 6-coordinate species usually exist in coordinating solvents. Because of their distinct absorption spectra, the two species may be selectively excited by monochromatic laser pulses. Upon excitation of the 6-coordinate ($^3B_{1g}$) form, the metalloporphyrin becomes temporarily trapped in the 6-coordinate $^1A_{1g}$ state. This is an antibonding situation due to the filling of the $d_{z^2}$ orbital, consequently the axial ligands temporarily dissociate. In weakly coordinating solvents such as pyridine, the equilibrium species is the 4-coordinate $^1A_{1g}$ state. The photoexcited molecule again becomes trapped in a metal d–d excited state, but now it is the 4-coordinate $^3B_{1g}$ state with a half-filled, low-lying, metal $d_{z^2}$ orbital. Thus, $\sigma$-donating ligands, such as nitrogenous bases, can now transiently bind.

The time scale of these excited-state transitions has been determined with transient absorption spectroscopy,[9-11] and in Figure 6 a diagram of the transitions is shown. In this scheme the decay via rapid radiationless processes of the Ni(PP) excited state from the higher levels (Q, B, etc.) having predominantly porphyrin orbital character to the lowest metal d–d states takes $<\sim 15$ ps.

When the ligated $^3B_{1g}$ species is excited (right side of diagram in Figure 6), rapid decay results in the formation of the "ligated" $^1A_{1g}$ state and subsequent loss of ligands in $\leq 35$ ps. On the other hand, excitation of the unligated $^1A_{1g}$ state results in the formation of the unligated $^3B_{1g}$ state in $\leq 15$ ps. The $^3B_{1g}$ state then persists for $\sim 250$ ps in the absence of strong ligands. However, in coordinating solvents, the unligated excited $^3B_{1g}$ state acquires ligands in $\sim 450$ ps. Both the transient unligated species (subsequent to excitation of 6-coordinate Ni(PP)) and the transient ligated species (subsequent to excitation of 4-coordinate Ni(PP)) persist for greater than 20 ns once they are formed.

**Transient Raman Spectroscopy of Nickel Protoporphyrin Complexes.** Time-resolved resonance Raman spectroscopy is a sensitive probe of the metalloporphyrin geometry and ligation state subsequent to the initiation of photochemistry. The equilibrium ground state resonance Raman spectra[11,12] (see Table I) of both 4- and 6-coordinate Ni(OEP) and Ni(PP) are well-known and provide a firm basis for the interpretation of our transient data. In particular, previous Raman studies have established the sensitivity of various "core-size" marker lines[5,36] ($\nu_2$, $\nu_3$, $\nu_{10}$) to changes in axial ligation. Moreover, the patterns of shifts resulting from porphyrin electron density changes,[37-39] ligation changes,[5,40-42] differences in metal electronegativity,[43,44] or alteration of metal spin state[38] are distinct from one another. In addition, specific structural information about the metal–axial ligand bond can be obtained from the transient Raman data.[5,42] Thus, the potential molecular information content of time-resolved Raman spectra far exceeds that of analogous absorption data.

The Raman spectra of Ni(PP) in coordinating solvents (Figures 1 and 2) clearly show that photoinduced ligation changes occur within the 10 ns laser pulse width. The appearance of the modes $^4\nu_{10}$, $^4\nu_3$, and $^4\nu_2$ at 1658, 1521, and 1594 cm$^{-1}$, respectively, in the spectra of Ni(PP) in pyrrolidine indicates an appreciable amount of photodissociation of the 6-coordinate ground-state species has occurred. The extent of observed photodissociation is both wavelength and power dependent. Photodissociation is observed with either 406- or 440-nm excitation. At the latter wavelength scattering from the 6-coordinate species is more resonantly enhanced (relative to the 4-coordinate species) whereas 406-nm excitation selectively enhances the 4-coordinate species. Thus, even though the 4-coordinate modes are of similar relative intensity at both excitation wavelengths, the fraction of 4-coordinate molecules is appreciably less in the 406-nm spectra.

At either wavelength the proportion of 4-coordinate species increases directly with laser power density. Since the ligand recombination half-life (>20 ns) is longer than the laser pulse, a linear increase in the proportion of excited-state species during the laser pulse is expected at 440 nm. Excitation at 406 nm produces a slightly more complicated situation since the photogenerated 4-coordinate molecules can, in principle, be excited by subsequent photons in the laser pulse. The proportions of 4- and 6-coordinate molecules will then be predicted upon the integrated solution (during the laser pulse width) of the differential rate equations involved in the excited-state kinetics and should be quite sensitive to the ratio of the rate constants for the formation of the two species. Obviously, our data presently allow us to make only qualitative comparisons.

The close similarity between the photophysics of Ni(PP) in coordinating solvents observed in this study and that of Ni(OEP) previously observed[13] argues strongly that the photodissociation (or photoassociation) of ligands is predicted upon metal-based excited states and that the decay pathways from porphyrin to metal d-orbital states are similar for the two molecules. Thus, our results corroborate the proposed photocycle of Holten and co-workers[9-11] and suggest that the initial excitation of the porphyrin $\pi$-system rapidly (<10's of ps) decays to a d–d bottleneck excited state where ligation changes may occur.

**Nickel Protoporphyrin Transients in Noncoordinating Solvents and Micelles.** Incorporation of Ni(PP) into detergent micelles provides useful models of monomeric 4-coordinate Ni(PP) in a hydrophobic environment. In this study nickel protoporphyrin was inserted into micelles of sodium dodecyl sulfate (SDS) and cetyltrimethylammonium bromide (CTAB). The equilibrium spectra of these species identifies them as being in the 4-coordinate form. Indeed, at low pulsed laser powers the spectra are identical with those obtained with low power cw laser excitation.[14,15] However, at high laser powers large changes are observed (relative to the equilibrium species) in the spectra obtained with both detergents (Figure 3).

At high powers (Figure 3b and c) there is a clear decrease in the relative intensity of $^4\nu_{10}$ (1662 cm$^{-1}$), $^4\nu_2$ (1597 cm$^{-1}$), and $^4\nu_3$ (1523 cm$^{-1}$) indicative of a decrease in the population of the 4-coordinate (ground state) species. Photoexcitation also produces a pronounced shift to lower frequency (1374–1376 cm$^{-1}$) and a broadening of $\nu_4$. The new modes which appear in the spectra occur at frequencies that are distinct from those observed for equilibrium 4-, 5-, and 6-coordinate Ni(PP) species. In particular, $\nu_{10}$ and $\nu_3$ appear at 1627–1630 and 1492–1495 cm$^{-1}$, respectively. These frequencies are significantly higher than those observed for the ligated $B_{1g}$ states of Ni(PP) in coordinating solvents.[14,15] Moreover, these effects are observed in both anionic (SDS) and cationic (CTAB) detergents. There are two possible explanations for the transient behavior of Ni(PP) in the micelles: (1) a very weak axial ligand is photoassociating subsequent to Ni(PP) excitation or (2) the observed spectra are those of the excited-state ($^3B_{1g}$) (Ni(PP) without bound axial ligands.

The fact that very similar behavior is exhibited by Ni(PP) in either anionic or cationic detergent micelles would appear to rule

(36) Spaulding, L. D.; Chang, C. C.; Yu, N.-T.; Felton, R. H. *J. Am. Chem. Soc.* **1975**, *97*, 2517.
(37) Yamamoto, T.; Palmer, G.; Gill, D.; Salmeen, I. T.; Rimai, L. *J. Biol. Chem.* **1973**, *248*, 5211.
(38) Spiro, T. G.; Streakas, T. C. *J. Am. Chem. Soc.* **1974**, *96*, 338.
(39) Spiro, T. G.; Burke, J. M. *J. Am. Chem. Soc.* **1976**, *98*, 5482.
(40) Shelnutt, J. A.; Straub, K. D.; Rentzepis, P. M.; Gouterman, M.; Davidson, E. R. *Biochemistry* **1984**, *23*, 3946.
(41) Shelnutt, J. A.; Dobry, M. M. *J. Phys. Chem.* **1983**, *87*, 3012.
(42) Asher, S. A. *Methods Enzymol.* **1982**, *76*, 731.
(43) Shelnutt, J. A.; Ondrias, M. R. *Inorg. Chem.* **1984**, *23*, 1175.
(44) Shelnutt, J. A. *J. Am. Chem. Soc.* **1983**, *105*, 774.

out the charged, polar head of the detergent molecules as possible axial ligands in this case. Water is a possible axial ligand for the transient Ni(PP) in these systems and has been shown to form weak complexes with other nickel porphyrin species.[45] While we cannot unequivocally rule out weak, transient ligation, the observation of similar transient behavior in Ni(OEP) and Ni(PPDME) in noncoordinating solvents (ref 46 and Findsen, Shelnutt, and Ondrias, unpublished results) leads us to conclude that the transient behavior of the Ni(PP)/micelle systems is not predicted upon ligand binding.

It is therefore likely that the 10-ns laser pulses create a significant amount of the unligated $B_{1g}$ excited state. This is not unexpected since time-resolved absorption studies have demonstrated that excitation to this state from an unligated $^1A_{1g}$ ground state occurs in $\leq$15 ps, whereas decay from the $^3B_{1g}$ state requires $\approx$250 ps in noncoordinating solvents.

The spectral properties of this excited-state species are of great interest since they represent the effects of the $d^2_{z^2} \rightarrow d^1_{x^2-y^2}$ transition upon the porphyrin. The most obvious effects are a substantial increase in porphyrin core-size. Previous studies[5] have established that the frequencies of both $\nu_3$ and $\nu_{10}$ are quite sensitive to porphyrin core-size. Their positions in the transient spectra indicate that the d–d transition alone engenders a core expansion from $\sim$1.95 to $\sim$2.02 Å. This is approximately two-thirds of the total expansion in going from equilibrium 4-coordinate Ni(PP) to equilibrium 6-coordinate Ni(PP). This is not unreasonable since the symmetry of the $d_{x^2-y^2}$ orbital allows it to interact directly with the porphyrin $\sigma$ system in an antibonding fashion.

The $\sim$10-cm$^{-1}$ shift to lower frequency of $\nu_4$ in the unligated $B_{1g}$ state further indicates a substantial redistribution of electron density in the porphyrin orbitals. This mode has been traditionally viewed as a sensitive indicator of the oxidation state of the central metal presumably because of its sensitivity to the degree of $\pi$-backbonding between the metal and the porphyrin $e_g(\pi^*)$ orbitals.[5] In this case, however, it appears that a substantial portion ($\sim$70%) of the frequency shift in $\nu_4$ between equilibrium 4- and 6-coordinate Ni(PP) results from the net d–d transition. This sensitivity to the population of the metal $d_{x^2-y^2}$ orbital probably arises from the increased pyrrole nitrogen–nickel bond distances of the expanded metalloporphyrin core which, in turn, leads to poorer overlap between the $d_\pi$ and porphyrin $e_g(\pi^*)$ orbitals. It should be noted that the relationship between the frequency of $\nu_4$ and the frequency of the core-size marker lines is similar to that observed for metal substitution.[43] Metal substitution effects on marker line frequencies appear to be based on differences in covalency of the porphyrin–metal bond for different metals. Thus, $\pi$ and $\sigma$ orbitals in addition to $e_g(\pi^*)$ and metal $d_\pi$ orbitals are probably involved.

**Photodynamics of NiMb and NiHb.** The Ni(PP) reconstituted globins contain unique species of Ni(PP) whose equilibrium properties have been well-characterized via conventional Raman techniques. In previous studies[14,15,32-34] it was established that all of the Ni(PP) sites in NiMb and approximately 60% of the Ni(PP) sites in NiHb are 5-coordinate. The stability of the 5-coordinate form of Ni(PP) in NiMb and NiHb and its photochemical behavior are of great significance. In solution there are few 5-coordinate Ni(PP) species that are stable.[16] Those that exist do so only at low concentration and in equilibrium with 4- and 6-coordinate forms. Stabilization of the 5-coordinate form is probably due to the steric constraints of the protein pocket surrounding the porphyrin. The addition of imidazole (Im) to a solution of NiMb does not appear to change the ligation state of the porphyrin. This may be indicative of a slightly out-of-plane nickel position in the Ni(PP) resulting from protein constraints upon the axial histidine position which inhibit the movement of the nickel into the porphyrin plane upon 6-coordination.

Nickel hemoglobin exists in an equilibrium between the 4- and 5-coordinate forms. This is probably a manifestation of the "tension" in the hemepocket that is caused by the quaternary conformation changes exhibited by hemoglobin. Numerous spectroscopic studies have confirmed that the hemepocket tertiary structure of Mb resembles that of Hb in an R-like conformation. Deoxyhemoglobin in phosphate buffer is in the T conformation. For iron hemoglobins the T-quaternary structure results in significantly weaker bonding interactions between the heme iron and the proximal histidine with the $\alpha$-chains possessing a weaker bond than the $\beta$-chains.[47-49]

Because NiHb like FeHb exists in the T structure,[32-34] one might also expect the nickel histidine bond to be weaker in NiHb than in NiMb. This is indeed the case as indicated by the $\sim$5-cm$^{-1}$ decrease in the nickel histidine stretching frequency for NiHb relative to NiMb.[14,15] It would also be reasonable to expect that the nickel hemoglobin $\alpha$-chains are more likely to possess 4-coordinate sites than either the nickel hemoglobin $\beta$-chains or nickel myoglobin.

Absorption studies of equilibrium Ni(PP) reconstituted globins indicate a progressive stabilization of 5-coordinate sites over 4-coordinate sites in the order Mb > HbA, $\beta_4$ tetramers > $\alpha^{SH}$ subunits.[32-34] Since the $\alpha^{SH}$ monomers and $\beta_4$ tetramers (both putative R-state structures) display equilibrium mixtures of coordination state, it is doubtful that the 4-coordinate sites in Ni(PP) reconstituted HbA are exclusively in the $\alpha$ subunits.[32]

The transient Raman data demonstrate that the photodynamic behavior of the nickel porphyrin is also greatly affected by its protein environment. In contrast to Ni(PP) model systems there is no evidence for any photodissociation of the proximal histidine in NiMb. At all laser powers and excitation wavelengths used the spectra remain exclusively characteristic of 5-coordinate Ni(PP). A similar situation is observed for the 5-coordinate sites of NiHb. However, if the 4-coordinate sites of NiHb are directly pumped (with 406-nm excitation), clear evidence of the photoinduced uptake of a fifth (but not sixth) ligand is observed in the growth of the relative intensities of $^5\nu_{10}$, $^5\nu_3$, and $^5\nu_2$ at 1623, 1488, and 1577 cm$^{-1}$, respectively, in the spectrum (Figure 5). Thus, the local protein environment modified the dynamic behavior of both 4- and 5-coordinate sites to a significant degree.

The apparent lack of photoinduced ligand dissociation at the NiHb and NiMb 5-coordinate sites is somewhat surprising in view of the behavior observed for the Ni(PP) and Ni(OEP) models. The three most likely explanations for this phenomenon are (1) 5-coordinate Ni(PP) is inherently inactive due to differences in decay pathways, between 5- and 6-coordinate species, (2) the 5-coordinate protein sites are in the dissociative $A_{1g}$ state but retain bound histidine due to constraints imposed by the proximal pocket, (i.e., the d–d transition does not occur on addition of the ligand), or (3) photodissociation does occur but religation is extremely rapid on a 10-ns time scale (cage recombination).

We believe that the first two possibilities are unlikely. The first scenario requires a gross rearrangement of decay pathways in 5-coordinate Ni(PP) relative to either 4- or 6-coordinate Ni(PP). While molecular orbital calculations[35,40] indicate that the relative energies of the metal $d_{x^2-y^2}$ and $d_{z^2}$ orbitals are affected by the number and $\sigma$-donor ability of the axial ligands, the basic excited-state structure of Ni(PP) remains similar in the 5- and 6-coordinate species. In the absence of any spectroscopically viable 5-coordinate Ni(PP) model complexes, this cannot be experimentally verified. However, there is no theoretical evidence that additional long-lived excited states or nonradiative processes exist in the 5-coordinate species. Moreover, the observation that the 4-coordinate NiHb sites are photoactive suggests that efficient pathways between $A_{1g}$ and $B_{1g}$ states exist even in the protein environment. The second possibility is untenable based upon recent magnetic susceptibility measurements which establish that the 5-coordinate sites in NiMb (and by analogy NiHb) are in the high-spin ($^3B_{1g}$) state at equilibrium.[50]

(45) Pasternack, R. F.; Spiro, E. G.; Teach, M. *J. Inorg. Nucl. Chem.* **1974**, *36*, 599.
(46) Cheung, L. D.; Yu, N.-T.; Felton, R. H. *Chem. Phys. Lett.* **1978**, *55*, 527.
(47) Nagai, K.; Kitagawa, T. *Proc. Natl. Acad. Sci. U.S.A.* **1980**, *77*, 2033.
(48) Nagai, K.; Kitagawa, T.; Morimoto, H. *J. Mol. Biol.* **1980**, *136*, 271.
(49) Ondrias, M. R.; Rousseau, D. L.; Kitagawa, T.; Ikedo-Saito, M.; Inubushi, T.; Yonetani, T. *J. Biol. Chem.* **1982**, *257*, 8766.

Since the expectation is that the excited state decay pathways of the 5-coordinate sites in NiHb and NiMb are qualitatively similar to that of the 6-coordinate Ni(PP) complexes, and that the ground state is $^3B_{1g}$, the apparent lack of photoinduced ligand loss must result from a specific alteration of ligand rebinding rates by the protein environment. The apparent time scales for the decay of photogenerated $^3B_{1g}(L)$ and $^1A_{1g}$ states can be used to infer the characteristics of the transition state between them (see discussion below).

It is significant that the 10-ns transient spectra of the NiHb 4-coordinate sites do not mimic those of 4-coordinate Ni(PP) in micelles. In particular, the behavior of $\nu_{10}$, $\nu_3$, and $\nu_4$ for the proteins clearly indicates the presence of a ligated $^3B_{1g}$ excited state. Thus, despite the protein constraints favoring 4-coordination in the equilibrium species, the excited-state species binds a single ligand on a time scale that is shorter than the 10-ns laser pulse width. This behavior clearly implies that the 4-coordinate Ni(PP) sites in NiHb are in a protein environment that provides a readily accessible nitrogenous ligand (most likely the hemepocket proximal histidine). The absence of photoinduced binding of a sixth ligand at the initially 4-coordinate sites almost surely results from the lack of a $\sigma$-donor ligand at a suitable orientation and/or proximity to the heme in the distal hemepocket.

**Transition-State Energetics for Photoinduced Ligation Changes.** Any attempt to explain the energetics and transition states involved in the photoinduced ligation changes of Ni(PP) must explain the following observations:

(1) For 6-coordinate Ni(PP) in coordinating solvents ligand loss and formation of the $^1A_{1g}$ state occurs in ~50 ps.[10] In solution, the reestablishment of the equilibrium between $^1A_{1g}$ and $^3B_{1g}(L_2)$ requires >20 ns although a diffusion-controlled process would require only ~20 ps. Clearly, an activation barrier exists for this process. Reasonable transition states are the unligated $^3B_{1g}$ state or the "ligated" $^1A_{1g}$ state (see Figures 6 and 7).

(2) In the 5-coordinate NiMb and NiHb sites, steric constraints of the protein on the imidazole's position and orientation apparently stabilize both the $^3B_{1g}(L)$ and the transition state relative to the $^1A_{1g}$ state. Thus, only a small energetic barrier exists for ligand rebinding and the ligand can rebind in a time approaching the diffusion-controlled limit of ~20 ps.

(3) The 4-coordinate sites in NiHb apparently behave in a manner analogous to the model nickel porphyrin in coordinating solvents, and a ligand is acquired in ~200 ps by the photogenerated $^3B_{1g}$ state. Thus, a measurable concentration of 4-coordinate sites converts to the relatively long-lived 5-coordinate form during the 10-ns pulse, and we observe an increase in the relative concentration of the 5-coordinate sites in NiHb. This clearly implies that the barrier between $^3B_{1g}(L)$ and $^1A_{1g}$ states is not significantly lowered relative to the $^3B_{1g}(L)$ state by the protein environment.

Figure 7 shows schematically a proposed decay mechanism resulting in transient ligation changes and return to the initial equilibrium state for excitation of the 4-coordinate and 5- or 6-coordinate forms in solution (solid lines) or in the protein matrix (dashed lines). The energies of the intermediate states are taken from the calculations of Ake and Gouterman.[35] These are the same as shown in Figure 6, except they are shifted by ~4 kT to qualitatively represent the equilibrium observed in NiMb.

Consider the photoexcitation of Ni(PP) in a coordinating solvent. Excitation of the equilibrium 4-coordinate ($^1A_{1g}$) species (Figure 7, upper left) results in the rapid creation of the $^3B_{1g}$ state which picks up ligands in less than a nanosecond. Excitation of 6-coordinate $^3B_{1g}(L)$ species (Figure 7, upper right) rapidly produces the $^1A_{1g}(L)$ species which then dissociates. Reestablishment of the equilibrium, between unligated $^1A_{1g}$ and $^3B_{1g}(L)$ states subsequent to photoexcitation, is, however, quite slow (>20 ns). This surely is a result of the transition state between $^1A_{1g}$ and $^3B_{1g}(L)$ being significantly higher in energy than either $^1A_{1g}$ or $^3B_{1g}(L)$. Two possible transition states for the interconversion between ground ligated and unligated states are the "unligated"

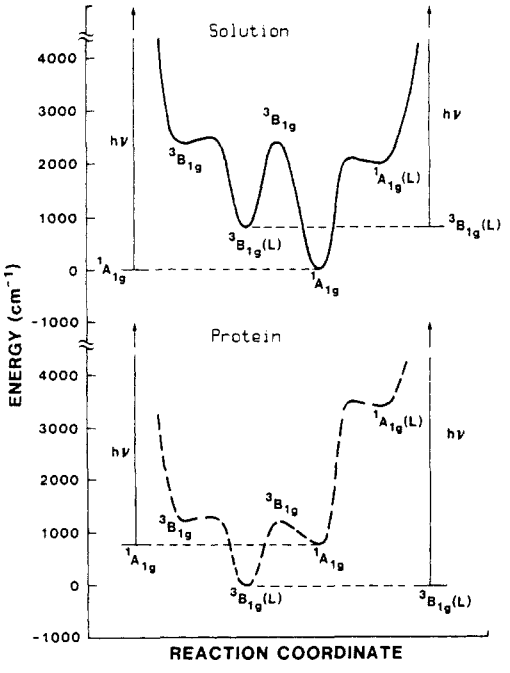


**Figure 7.** Hypothetical picture of relaxation of photoexcited 4-coordinate (left) and 5- and 6-coordinate (right) nickel porphyrins in solution (top) and the effect of the protein matrix (bottom). The state energies used are the same as in Figure 6 but shifted by ±4 kT. State energies are taken from calculations of Ake and Gouterman[35] with the $^3B_{1g}$–$^1A_{1g}$ energy gap taken as 2500 cm$^{-1}$ for 4-coordinate (in plane) complex and −2000 cm$^{-1}$ for 5-coordinate nickel (out-of-plane) with one basic ligand; thus, binding of the ligand lowers the triplet manifold by about 4500 cm$^{-1}$ with respect to the singlet manifold. The protein matrix is assumed to lower the energy of $^3B_{1g}$ state by 800 cm$^{-1}$ (≈4 kT) and raise the $^1A_{1g}$ state by 800 cm$^{-1}$ thereby shifting the equilibrium in favor of the ligated sites (dashed line). Thus, the unligated species is favored by 800 cm$^{-1}$ in solution (solid lines); the ligated species is favored by 800 cm$^{-1}$ for the protein. We assume the protein has a larger effect on the energies of the unligated $^3B_{1g}$ state and the "ligated" $^1A_{1g}(L)$ level.

$^3B_{1g}$ state and the "ligated" $^1A_{1g}$ state. Thus, the transition state between the $^3B_{1g}(L)$ and $^1A_{1g}$ states of Ni(PP) in solution is probably a mixture of these two states. In Figure 7 we use the $^3B_{1g}$ level as the maximum of the barrier between the equilibrium species.

Within the protein matrix (dashed line, bottom) the energetics of the transition between $^3B_{1g}(L)$ and $^1A_{1g}$ are obviously greatly modulated. Our data indicate that the transition state is considerably stabilized relative to the $^1A_{1g}$ state but remains significantly destabilized relative to the $^3B_{1g}(L)$ state (vide supra). These observations are easily rationalized by the energy diagrams in Figure 7. The close proximity of the axial ligand in the protein environment would be expected to stabilize the "unligated" $^3B_{1g}$ state and destabilize the $^1A_{1g}(L)$ state relative to solution conditions. Moreover, if the transition state is predominately $^3B_{1g}$ in character both it and the $^3B_{1g}(L)$ state would be stabilized to approximately the same extent. This scenario would lead to the observed increase in the rate of ligand recombination ($^1A_{1g} \rightarrow {}^3B_{1g}(L)$) without increasing the rate at which photogenerated $^3B_{1g}(L)$ sites convert to $^1A_{1g}$ sites in the protein. A predominately $^1A_{1g}(L)$ transition state is inconsistent with our data since it would lead to slower rates for both these processes and the observation of photogenerated $^1A_{1g}$ sites in the 420-nm excitation spectra of NiMb.

The above arguments lead us to conclude that within the protein matrix, the transition state for the activated process $^1A_{1g} \leftrightarrow {}^3B_{1g}(L)$ is primarily of "unligated" $^3B_{1g}$ character. If this is true, then the spectra of $^*B_{1g}$ species generated from Ni(PP) in micelles directly probe the characteristics of the transition state controlling the ligation dynamics in the proteins.

**Comparisons of the Photodynamics of FeHb and NiHb.** The comparison of the photodynamics of the 5-coordinate Ni(PP) sites in NiHb and NiMb with those of the native ferrous hemoproteins

(50) Rifkind, J. M. et al., manuscript in preparation.

is of considerable interest. The photolysis of exogenous ligands (CO, $O_2$, NO) from HbA and Mb has been extensively studied via transient Raman and absorption techniques.[4-7] While photodissociation of the exogenous ligand has been found to be a relatively efficient process over a broad spectrum of excitation wavelengths, no evidence for photolysis of the bound proximal histidine has been found in either equilibrium 5- or 6-coordinate hemoproteins (deoxy and ligated hemes, respectively). No transient 4-coordinate Ni(PP) species is observed in NiMb (and at the equilibrium 5-coordinate sites of NiHb). We have interpreted this as resulting from rapid (on a nsec timescale) protein-facilitated recombination kinetics subsequent to ligand photolysis. However, on a picosecond time scale we expect that photolysis of the proximal histidine in NiHb and NiMb may be evident in their transient Raman spectra (vide supra). On the other hand, transient spectroscopy with ≤50 ps time-resolution[17,20,21,24,25] has failed to reveal any photolysis of the proximal histidine in HbA and Mb. Thus, the apparently similar behavior of 5-coordinate Ni(PP) and Fe(PP) sites in Hb and Mb upon photoexcitation arises from different origins.

While photodissociation of the proximal histidine is expected for NiHb and NiMb on the basis of the behavior of nickel porphyrin models, the behavior of iron protoporphyrin model complexes would not lead one to anticipate photodissociation of the proximal histidine in ferrous Hb and Mb. A recent picosecond transient absorption study of ferrous 6-coordinate Fe(PP) by Dixon et al.[51] demonstrates that the photodynamics of Fe(PP) are markedly different from those of Ni(PP). They found that only a single axial ligand was released upon photoexcitation of 6-coordinate Fe(PP) in coordinating, basic solvents. Moreover, no ligand dissociation was observed in 5-coordinate $Fe^{II}$(PP)(2-MeIm) models. Dixon et al. concluded that the dissociative excited state observed in 6-coordinate Fe(PP) arises from either $d_\pi \rightarrow d_{z^2}$ or porphyrin $\pi \rightarrow d_{z^2}$ transitions. This results in the promotion of a single electron to the previously unfilled $d_{z^2}$ orbital and dissociation of only a single nitrogenous ligand. An earlier excited state ($\tau \approx 35$ ps) was also observed in Fe(PP) models[51] and postulated to result from a $^3T$ ($\pi,\pi^*$) excited state of the porphyrin. This state would not be expected to perturb porphyrin core-size to the extent of the $d_{z^2} \rightarrow d_{x^2-y^2}$ transition evident in Ni(PP) but might have a larger effect upon the frequency of $\nu_4$. The extrapolation of the photolytic behavior of Fe(PP) model complexes to CO or $O_2$ bound hemes in hemoglobin is not straightforward since the exogenous ligands exhibit substantial $\pi$-electronic interactions with the heme iron that are absent with nitrogeneous ligands. However, such behavior might account for the observed photolysis of exogeneous ligands and not the proximal histidine in HbA and Mb. Thus the impressive cage recombination effects exerted by the protein matrix in NiHb and NiMb are not evident in the iron proteins.

(51) Dixon, D. W.; Kirmaier, C.; Holton, D. *J. Am. Chem. Soc.* **1985**, *107*, 808.

## Summary

This study demonstrates that transient resonance Raman scattering can be used to probe the molecular details of the excited state photodynamics of Ni(PP) in a variety of local environments. Our spectra confirm the observations of previous transient absorption studies of Ni(PP) in coordinating solvents and reveal the effects of photoexcitation upon porphyrin structure and ligation state. The photodynamics of Ni(PP) incorporated into micelles and noncoordinating solvents is markedly different from that of Ni(PP) in coordinating solvents. During pulsed laser excitation, an appreciable population of a species having a distinctive Raman spectrum unlike that of equilibrium 4-, 5-, or 6-coordinate Ni(PP) is created. This is most likely the spectrum of the unligated $^3B_{1g}$ state of Ni(PP) and allows for the deconvolution of the effects of the $d^2_{z^2} \rightarrow d^1_{x^2-y^2}$, $d^1_{z^2}$ transition from those engendered by ligation. Finally, we have shown that the local protein environment in Ni(PP) reconstituted Hb and Mb exerts a pronounced effect upon the proximal histidine photoinduced ligation kinetics of Ni(PP). The protein constraints evidently stabilize the ligand binding transition state in both the equilibrium 4- and 5-coordinate site, thus facilitating the photoassociation of the proximal histidine in the former and greatly increasing the recombination rate of the photodissociated histidine in the latter.

**Acknowledgments.** We thank Dr. J. M. Rifkind for communication of results before publication and Prof. D. Holten for thoughtful comments and stimulating discussion.

**Registry No.** Ni(PP), 15415-30-2.